

Design and fabrication of a novel three wheel robot with a SLE based lifting mechanism and line tracking capability

Shameek Ganguly¹, Akash Garg², Akshay Pasricha¹ and S.K. Dwivedy^{1*}

¹ Department of Mechanical Engineering, Indian Institute of Technology Guwahati, India

² Department of Civil Engineering, Indian Institute of Technology Guwahati, India

*Corresponding Author (email: dwivedy@iitg.ernet.in)

Abstract

The present paper deals with the design and development of a modular three wheel robot capable of autonomously navigating a structured environment by means of tracking a curved line on the floor. Furthermore, it is equipped with a deployable scissor lift with an end effector plate thus providing applicative modularity to the robot. The main application is envisaged to serve as an automatic guided vehicle in industries such as automotive and construction where cost effectiveness is an essential criterion for automation and mobility is a highly desirable functionality. Mechanical design is carried out using stress analysis with the help of the finite element software package ANSYS and velocity response curves are generated for the highly non-linear motion of the scissor lift. Finally an algorithm is developed for high speed line tracking using LED and phototransistor pairs and results are presented in terms of experimental data as well as simulated responses.

1. Introduction

Industrial robots have been used widely for automation in varied fields such as manufacturing and assembly for several years now. More recently the development of Automated Guided Systems has resulted in the induction of autonomous mobile robots in the industrial scenario which have been successfully used for fulfilling roles such as in logistics and materials handling ([1-3]). A wide amount of scientific literature has been devoted to the study and development of more intelligent AGV systems ([2-4]). At the same time, a lot of work has been directed towards the development of intelligent navigation systems which allow maximum workspace adaptation and flexibility ([5-7]). Similarly, work has also been directed towards the development of improved ultrasonic and optical or vision based sensors for compatible utilization with the advanced navigation guidance systems ([6-8]).

However, these techniques have so far been restricted to simple robots only for the task of transportation.

The main motivation of the present paper lies in the mobilization of application based industrial robots and its induction into an AGV system. Furthermore, the present work proposes to modularize the application specific end effectors thus allowing development of truly 'modular AGVs'. Design concepts of modularity are very cost-effective and have attracted vast scientific research with applications including the development of industrial as well as non-industrial robots. The current work achieves a basic degree of modularity by means of providing a plug and play facility for several types of end-effectors which can be mounted over an end-effector plate which is further clamped on a scissor lift. Scissor lifts are pantograph-based deployable lifts ([9,10]) which allow large magnification over original dimensions similar to multi-joint articulated booms but are naturally better conditioned against failure ([10]). Their highly non-linear kinematics and dynamics have been discussed using several approaches in other scientific papers ([9,10]).

Furthermore, the use of deployable structures coupled with the modularity of the AGV allows for highly efficient idle docking and transportation in a very compact form and at the same time, opens up applications such as construction (or other automated activities) in areas with bottle-neck openings like mines, sewers, pipelines and tunnels. In the present case motion is achieved using a simple two wheel independent drive system but can be easily extended to four or more wheeled differentiable drive as has been devised in [11]. Moreover, using advanced hybrid locomotive techniques ([12]), the concept can be extended to unstructured environments for use in construction industries where difficult terrain such as steps and ledges are often encountered.

Navigation and guidance support systems for AGVs have been discussed in a vast amount of scientific review literature and have come up with solutions ranging from the use of magnetic tapes on flooring to 3D vision based self-supported navigation ([1,5,7,13]). However, high initial uptake cost has restricted the practical use of navigation systems for AGV systems in industries to simple ones such as guided wire system or magnetic tapes

or painted lines on the floor ([1,8]). The current work deals with the problem using the latter of these approaches by suggesting a highly restructure-able solution using tapes with colors contrasting to that of the workshop floor. The presently designed robot is equipped with minimal electronic hardware for the detection of this line and makes up for the demands for high accuracy using a hybrid PID ([14]) and geometrical algorithm for the task. An array of three LED and phototransistor pairs is used to detect and track the line in order to demonstrate a minimal cost performance but can be easily extended to larger arrays of detectors as has been done in [8]. Further research is also suggested over the use of 2D cameras for this purpose which has been successfully applied in [13].

2. Design

2.1 Design principle of the robot

The current robot is an independent two-wheel drive type device mounted with a scissor lift and an end-effector plate, along with necessary electronic control and power supply. Its motion is restricted to the plane of the structured workspace normal to the direction of gravity in order to neglect its effect on spatial velocity. An optimized CAD model of the robot has been prepared and is shown in Fig.1.

As this work is intended to be a first step towards the development of a truly modular automatic guided robot, those design aspects which support the modularity of the robot are of special interest.

2.2 Modularity

In the present work, modularity of the robot is defined as the ability of an autonomous mobile industrial robot to be used as a *multi-purpose worker* in a pre-defined environment, which is achieved by the following principles:

2.2.1 Hardware Plug n Play

This feature deals with the easy hardware interface between the base robot and any unknown class of end-effectors. This primarily includes two main issues which are the support mount for an end-effector of unknown base dimensions and any other auxiliary hardware support that may be required for it. The present work achieves this by providing a specially designed end-effector plate.

2.2.2 Control System modularity

This feature refers to the easy control system interface for an end-effector by providing electronic control support as well as software abstraction for easy control of the device.

Electronic control of the end-effector is interfaced with the main control system of the robot by means of easily adaptable I/O ports.



Fig.1 CAD Drawing of the Vehicle

The present work uses software abstraction by providing inbuilt functions for the basic control of the robot, which may be used to quickly write more complex routines for operational control of the end-effector (further details in section (2.3.2)).

2.2.3 Architectural Modularity

This feature refers to the support provided by the overall architecture of the base robot for increasing the efficiency of any end-effector. For the present work a scissor lift is used to increase the range of any unknown class of equipment mounted on the robot by a significant amount in the direction perpendicular to the plane of motion of the robot itself. Being a deployable pantographic mast, it has several factors of advantage over the traditional boom or crane lifts ([10]) and obviously, over a constant height mount for the end-effector. Its design is discussed at length in the following section.

2.3 Key Hardware Design Aspects

2.3.1 Scissor Lift

The current lifting mechanism (scissor lift) is based on a planar parallel operated pair of deployable mast created by interlinked Scissor Like Elements (SLEs). The Scissor like elements consist of two metallic rods connected parallelly with a revolute joint at their centres. Two SLE's are interlinked by pinning two free ends of one unit with two of the other in such a way that the planarity of the structure is maintained along with the fore-mentioned constraints.

The maximum height reached by a scissor lift with N SLE's shall be N times the maximum height reached by a lift with a single SLE. Similarly, the dead weight of a lift with a single SLE shall be multiplied by a factor of N . The parallel between the two separate planar lifts is maintained by horizontal connecting rods. The number of SLE's used in each planar lift is the same to maintain the lifting plane at a perpendicular to both the planar lifts. This lifting plane in the current model is occupied by a grab plate which is designed so as to support several types of end-effectors to suit industry-specific requirements (section (2.3.2)). This metal plate is supported by means of revolute pinned joints on one edge and rollers on the other. Similarly, the lift is supported by two revolute joints at one edge on the base and two guided rollers on the other edge.

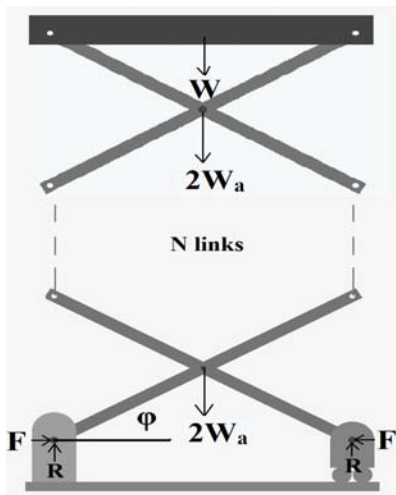


Fig 2 Free body diagram of system

For the present work, the dimensions of the designed scissor lift have been determined using the governing equation for such structures for similar link dimensions. From free body diagram shown in Fig. 2 one can write

$$F = (W + (N \cdot W_a)) / \tan \phi, \quad (1)$$

where F is the force applied by the actuator, W is the net load on the scissor lift inclusive of the weight of the end-effector plate, W_a is the weight of each link in the system N is the number of links in the system and ϕ is the angle between the bottom most link of the scissor lift and the base of the robot.

The required working conditions constrained the minimum extension of the scissor lift from its collapsed state to its completely extended state to a ratio of 1:4. Furthermore, the maximum payload was set to be 7kg. With these working constraints, the model of the scissor lift was developed on the FEM package ANSYS using large displacement small-strain formulations and BEAM188 structural elements. Frictional effects at the contact pins have been neglected for simplicity. All pins

have been considered to be rigid under working assumptions. The dimensions of each link was then optimized to avoid Euler buckling failure as well as bending due to moment at the mid-point of each link. The scissor lift consists of 14 links on each side made of aluminum, each of length 32.4cm with the cross-section as shown in Fig.3.

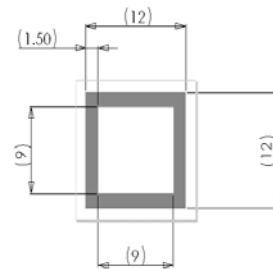


Fig.3 Cross-Section of Link
 (All dimensions are in mm)

The lift is powered by a lead screw mechanism (pitch 3mm) using a standard wiper motor with driving torque of 23.7 N-m based on above discussions. Discussion on the highly non-linear kinematics which govern the control of the lift is to be found in section (3.1.3).

2.3.2 The End-effector Plate

The end-effector plate is supported on top of the scissor lift and lies in its lifting plane as presented in Fig.4. It consists of a metal plate equipped with two support clamps which can be bolted to position on a guided linear rail. This allows for an adjustable distance between the two clamps which are envisaged to act as mount supports for an end effector. A complimentary support is provided for adjusting the dimensions of the mount in the direction of motion of the robot. Together, the mount clamps and the frontal support form the basis for the basal rigid support to any end-effector due to their in-plane dimensionally adjustable nature.

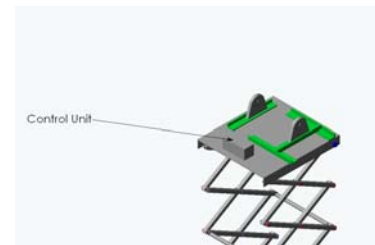


Fig.4 The End Effector Plate

Additional modularity for the control of the end-effector is achieved by providing a terminal for power-supply (which is limited by the onboard power supply) and

control I/O ports for interfacing with the main control system of the robot, in a control housing box, mounted on top of the end-effector plate.

3. Control System and Navigation

3.1 Control System Architecture

For efficient and cost effective control of the proposed AGV the present work has used high performance and low power Atmega series microcontrollers based on the AVR RISC architecture. Depending on the accuracy and speed of operation required the clock speed can be selected ranging from 1 MHz to up to 8MHz. The In System Programmable flash (ISP) was programmed through an SPI serial interface using a conventional non volatile memory AVR USB programmer compatible with Atmel's STK500V2 with implemented USB to serial converter to provide high speed USB based programming with the help of a standard PC, thus enabling quick programming of additional motions of the end-effector.

For easy development the current work uses an AVR development board, the salient features of which are as follows:

1. Power regulation and filter circuit: Ensures a 5V constant spike free supply for the microcontroller and a 12V supply for the actuators.
2. Serial programming header: For easy in-system programming of the microcontroller circuit.
3. Standard ports: For connecting the external components such as the sensors and motor drivers.
4. UART link header: Provides a serial link between the microcontroller and external devices such as a PC or a LCD for displaying data.

Lead acid batteries are used as a power source for the AGV. It is important to have different power sources for the actuators and the microcontrollers as sudden switching on of an actuator can sometimes cause the battery voltage to momentarily dip resulting in resetting of the microcontroller if it uses the same power source.

3.1.1 Sensor Architecture

For sensing the position of the line accurately the sensors need to distinguish between the background and foreground color. The current work uses analog optical sensors for this purpose which use the intensity of light reflected back from a surface to infer its color. These sensors use high intensity red color LEDs for illumination and a direction phototransistor for line sensing. The phototransistor has a convex lens precisely aligned with it that gives it a very small viewing angle of just about 5 degrees. This makes the sensor highly immune to ambient

light. However, to ensure dead-spot accuracy as required for industrial purposes, additional ambient light guard is added. To ensure proper following of the line an array of 3 such sensors is used as shown in Fig.5. When the robot is not on a white line the amount of light reflected is less and the phototransistor remains in the active state giving a high output voltage. When on a white line the reflected light drives the phototransistor into saturation resulting in a low output voltage.

However for proper operation of the line following algorithm it is very important to calibrate the sensors suitably in the working environment.

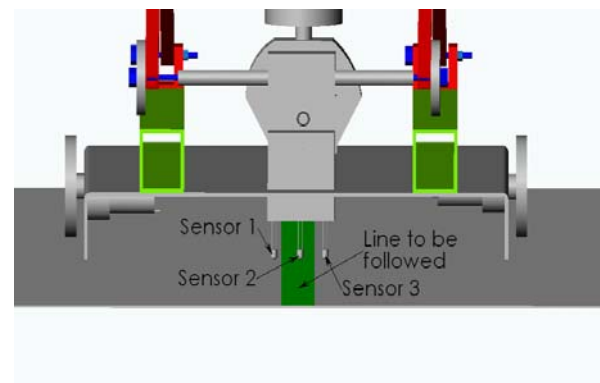


Fig. 5 Front view of the robot base showing the arrangement of sensors with respect to the line

3.1.2 Motor Control Architecture

The current work uses high torque geared DC motors for driving the AGV. These motors are controlled by using a dual H bridge module

The speed of the motor is controlled by varying the supply of power to it using Pulse Width Modulation (PWM). PWM uses a square wave whose pulse width is modulated resulting in a variation in the average value of the waveform. This variation in average value of the waveform results in a corresponding change in the power supplied to the motor. The current work uses the microcontroller to generate the PWM signal. The speed of the motor can be varied by simply modifying the value of a counter in the microcontroller. This feature is coupled with the motion control of the robot to achieve smooth and flexible motion and turn negotiation even at high speeds.

3.1.3 Scissor Lift Control

The linear motion of the deployable scissor lift is controlled by a high torque DC motor, the speed of which is controlled using PWM and direction with an H bridge circuit. For efficient use of the proposed AGV it is essential to accurately control the position and velocity of the end effector attached to the tip of the deployable

scissor lift. However the non linear kinematics and dynamics of such pantograph structures [15] make it a challenging task to do so. For a simple single link scissor lift structure such as that shown in Fig.2, if a constant force is applied at the basal roller joint the non linear velocity vs. motion time response is as shown in Fig.6. These curves are generated using ANSYS and agree with the experimental observations. A closed-loop feedback control is used to quantify the force applied at the basal joint and hence maintain the velocity of the end effector at a constant value. The feedback is represented by the angle ϕ in Fig.2. This angle can be measured with the aid of an encoder. Using analytical methods [15], the present work calculates the force to be applied at the basal roller joint as a function of the feedback angle for maintaining the end effector at a constant velocity. The function is illustrated by the graph in Fig.7 for a sample situation.

3.1.4 Software Modularity

The software that drives the proposed AGV is modularized by presenting several inbuilt functions which render the lower level hardware and software information to be abstract in nature. Some of these functions are given in this section.

Direction and speed control for the AGV:

This function controls the direction and speed of the AGV. The inputs to this function are the required speed v , the turning angle χ and a factor determining the turn speed given by ε . This factor smoothly maps the turning radius ψ to a value between 0 and 1, where $\varepsilon = 0$ denotes an instantaneous turn while $\varepsilon = 1$ represents a very large turning radius. Any continuous mapping is permissible and is purely a user-based choice. For the current work, it has been defined as:

$$\varepsilon = 1 - \exp(-A \cdot \psi) \tag{2}$$

where A is a constant of unit magnitude such that the product $A\psi$ is a non-dimensional quantity. Fig.8 shows the directional motion of the centre of mass of the robot during the turn. \hat{n}_1 and \hat{n}_2 are spatial unit vectors pointing in the direction of the robot before and after the turn respectively. The algorithm further makes use of PWM for achieving the desired motion.

Direction and speed control of the scissor lift:

This function is used to control the motion of the scissor lift. In the constant velocity mode the velocity v at which the lift rises and the direction χ are taken as the input argument. The user has to ensure that the velocity is within the limits of physical constraints. The user should set χ to 1 for the lift to go in the upward direction and to -1 for the lift to go in the downward direction. The algorithm is given in next subsection.

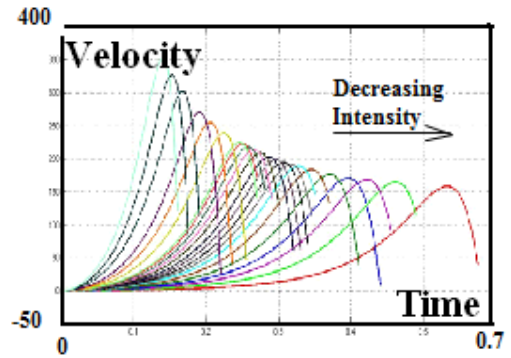


Fig. 6 Velocity distribution over time for various applied intensities at the base of the scissor lift

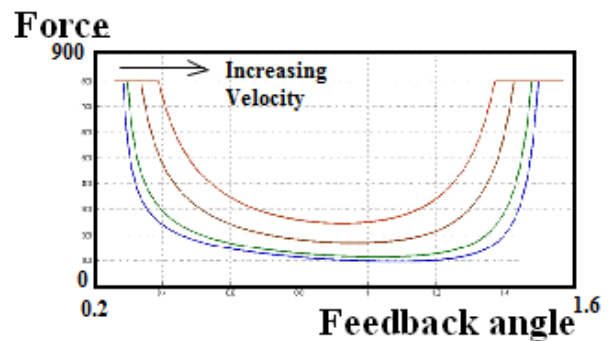


Fig. 7 Force as a function of feedback angle for various uniform velocities of the end-effector plate

The algorithm applies a force corresponding to the feedback angle for the input velocity by using a function such as that shown in the graphs in Figs.6, 7.

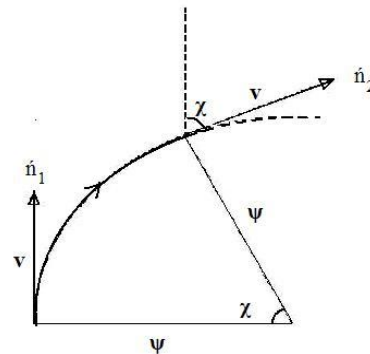


Fig.8 Directional properties of a turn of the robot

3.2 Navigation

3.2.1 Line Tracking

Error estimation in line tracking has been performed in [8] using parameters θ which is the angle between the longitudinal orientation of the robot and the local tangent

to the line and Γ which is the positional error of the robot with respect to the center of the line. However it is trivial to prove that such an estimate is not possible in the minimal restrictive case presented in the present work using a linear array of three sensors. Instead, a representational error in terms of the seven possible states of the sensory distribution over the line to be tracked is used as an input to the hybrid geometrical PID algorithm detailed in the following section. There are five possible primary states of the system, wherein any one or two of the sensors 'sense' the line. Additionally, there exist two hybrid cases which result in ambiguous state function. They involve either all of the sensors returning low output or all of them returning high output. The former case represents a case of overshoot and is resolved by a geometrical algorithm. The latter case is simply a case of oblique re-entry if the distance between the wing sensors is more than the width of the line as in the present work and is resolved by the PID algorithm.

The following three parameters are used to describe the state of the system:

L , M and R denote the ADC converted digital signal of the left, middle and right sensors respectively where a signal is considered *high* in case of detection of line and *low* if not.

3.2.2 Hybrid Geometrical PID Algorithm

The proposed algorithm is a variation of the PID algorithm for line following based on the analysis of the input state $f(L, M, R)$. The representational state is described by the following formula:

$$f(L, M, R) = \omega_M \cdot (1 - M) + \omega_W \cdot |R - L| \quad (3)$$

where ω_M and ω_W are positive weighting numbers associated with the middle sensor and the wing sensors respectively

The error ζ in the system as derived from the state is given by:

$$\zeta = k^{-1} \cdot f(L, M, R) \cdot (L + M + R)^{-1} \quad (4)$$

where k is the smoothness constant of the algorithm. A high value of k results in a slower but smoother tracking as the input error to the PID algorithm is low resulting in smoother corrective turns of the robot. On the other hand, a smaller value results in faster tracking with increased maximum deviation due to jerky turns at high speeds. In practical usage, k is nothing but the inverse of the proportional error control parameter of the algorithm itself and may hence be excluded.

The third factor in Eq. (4) is the hybrid check factor which checks for the hybrid case of overshoot.

Furthermore, τ is defined as the a reference period of time for which the robot may be allowed to run for a minimum permissible distance (d) with both wheels

rotating in similar sense, in a single loop of the algorithm without compromising on accuracy.

$$\tau = d / v(t) \quad (5)$$

where $v(t)$ is the instantaneous speed of the robot which may be either measured by encoder feedback or be an average calibrated parameter for a given input voltage. Using Eqs. (3-5) the proposed algorithm can be outlined as follows:

```
// start control loop
1. Input sensor values  $L, M, R$ 
// Nomenclature of non_trivial parameters:
//  $kp$  = proportional error control parameter
//  $ki$  = integral error control parameter
//  $kd$  = differential error control parameter
//  $(p, i, d)$  = representational error values in PID control algorithm
//  $pre\_zeta$  = error from previous run
// straight run = both wheels of robot move in similar sense to enable forward motion
// left turn = differential left turn with left wheel stationary in robot's local reference frame
// right turn = differential right turn with right wheel stationary in robot's local reference frame
// on-the-spot turn = differential turn executed by rotating both wheels in opposite sense
//  $abs(x)$  = absolute value of  $x$ 
2. Evaluate state  $f(L, M, R)$ 
3. Evaluate error  $\zeta$ :
if  $\zeta$  is zero set  $\zeta$  equal to  $pre\_zeta$ 
if  $\zeta$  is infinite reset  $\zeta$  and set overshoot_flag
4. Evaluate PID configuration:
 $p = kp \cdot \zeta$ 
 $i = ki \cdot (i + \zeta)$ 
 $d = kd \cdot (\zeta - pre\_zeta)$ 
 $PID\_parameter = p + i + d$ 
if  $pre\_zeta$  is zero invert sign of  $PID\_parameter$ 
//Asymptotic re-entry onto line
5. Set  $pre\_zeta$  to be equal to current  $\zeta$ 
6. Motion control
if overshoot_flag is reset
    Evaluate  $run\_time = \tau / abs(PID\_parameter)$ 
    if  $PID\_parameter$  is zero
        run straight for time  $\tau$ 
    else
        //Slight errors in trajectory
        if  $PID\_parameter$  is negative
            left turn for time given by  $run\_time$ 
        else
            right turn for time given by  $run\_time$ 
if overshoot_flag is set
//Execute hybrid geometric algorithm for asymptotic line re-detection
Evaluate  $run\_time = \tau \cdot abs(\mathbf{i})$ 
Evaluate  $secondary\_run\_time = \tau \cdot \eta$ 
```

// η is an experimentally calibrated parameter which depends on the ratio of the overshoot to the speed of the robot

if $i < 0$ *on-the-spot left turn* for time given by *run_time*
 right turn for time given by *secondary run_time*
 if $i > 0$ *on-the-spot right turn* for time given by *run_time*
 left turn for time given by *secondary run_time*

//It is theoretically impossible for i to be zero in cases of overshoot
 //repeat loop until destination is reached.

4. Results

4.1 Simulation

To simulate the high speed line following of the developed robot a MATLAB code has been developed and the simulation results are shown in Fig. 9 and Fig. 10. As shown in Fig. 5, the robot has three sensors for tracking the line. Based on its working dimensions from section(2.3.1), the velocity of the robot is considered to be 1m/s. The middle sensor is assumed to coincide with the COG (center of gravity) of the robot. Based on the algorithm given in section 3.2.2, Figure 8 shows the working of the robot on a 45 degrees sharp turn on a line.

Figure 10 shows the asymptotic re-entry of the robot into the line after moving out of it completely due to high speed.

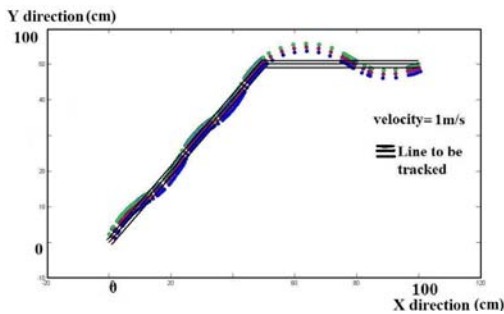


Fig.9 Rendering a 45 degrees turn (scale of length in cm on both axes, direction of travel from left to right)

4.2 Fabrication

The proposed robot has been fabricated in workshop of Mechanical Engineering Department, IIT Guwahati, using standard lathe and milling machines. The photographs of the fabricated robot are shown in Fig.11 and Fig.12. Aluminum channel sections are used in the fabrication of the robot due to its light weight and adequate tensile strength. Based on the mentioned algorithms experiment has been performed, and the robot has successfully tracked the desired path with straight lines and bends.

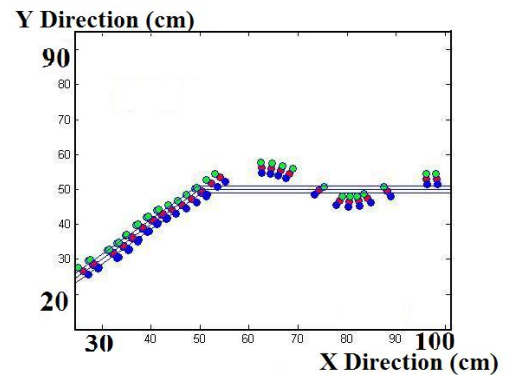


Fig.10: 45 degrees turn- asymptotic re-entry to line



Fig.11 Fabricated scissor lift



Fig.12 Robot Base

5. Conclusions

In the present work, a SLE based lifting mechanism is designed and fabricated for lifting a load of upto 7 kg. It also encompasses the groundwork for the development of a modular AGV for working in structured industrial

environments. It supports hardware as well as software and architectural modularity in terms of the use of an unknown class of end-effector in conjunction to its pre-equipped scissor lift by means of a specially designed end-effector plate and software abstraction. Furthermore, it is equipped and programmed electronically for high speed line following using a novel geometrical PID algorithm. It is envisaged that such a class of robots will immensely reduce prices of industrial robots and usher in the usage of truly multi-purpose robots in the industry. Thus the present work is important in terms of laying a primary foundation for the development of architecturally more advanced 'modular AGVs'.

Acknowledgements

The authors gratefully acknowledge the financial support given by Department of Mechanical Engineering, Indian Institute of Technology, Guwahati.

References

- [1] L. Schulze, A. Wullner, "The Approach of Automated Guided Vehicle Systems," *IEEE International Conference on Service Operations and Logistics, and Informatics*, pp.522-527, 21-23 June 2006.
- [2] D. Y. Lee, F. DiCesare, "Integrated scheduling of flexible manufacturing systems employing automated guided vehicles" *IEEE Transactions on Industrial Electronics*, Vol. 41, No.6, pp 602-610. December 1994.
- [3] A.F. Kahraman, A. Gosavi, K.J. Oty, "Stochastic modeling of an automated guided vehicle system with one vehicle and a closed loop path", *IEEE Transactions on Automation Science and Engineering*, Vol. 5, pp 504-518, July 2008.
- [4] N. Wu, M. Zhou, "Modeling and Deadlock Avoidance of Automated Manufacturing Systems With Multiple Automated Guided Vehicles" *IEEE Transactions on systems, Man and Cybernetics* Vol. 35, No. 6, pp. 1193-1202, December 2006.
- [5] E. M. Petriu, "Automated guided vehicle with absolute encoded guide-path" *IEEE Transactions on Robotics and Automation*, Vol. 7 No. 4, pp562-565, August 1991.
- [6] A. Kelly, B. Nagy, D. Stager, R. Unnikrishnan, "An Infrastructure-Free Automated Guided Vehicle System Based on Computer Vision" *IEEE Robotics and Automation Magazine*, pp. 24-33, September 2007.
- [7] Z. Katz, G. Bright, "A Guidance Technique for an Automated Guided Vehicle" *International Journal of Advanced Manufacturing Technology*, Vol. 7, pp198-202, 1992.
- [8] G. A. Borges, A. M. N. Lima, G. S. Deep, "Characterization of a Trajectory Recognition Optical Sensor for an Automated Guided Vehicle" *Transactions on Instrumentation and Measurement* Vol. 49 No. 4 pp. 813-819, August 2000.
- [9] J.S. Zhao, F. Chu, Z.J. Feng, "The Mechanism Theory and Application of Deployable Structures Based on SLE" *Mechanism and Machine theory*, Vol. 44 pg. no. 324-335, 2009.
- [10] C. Gantes, J. J. Connor, R. D. Logcher, "Simple Friction model for Scissor type Mobile Structures" *Journal of Engineering Mechanics*, Vol. 119 No. 3 pp 456-475, March 1993.
- [11] L. Beji, Y. Bestaoui, "Motion Generation and Adaptive Control Method of Automated Guided Vehicles in Road Following" *IEEE Transactions on intelligent transportation systems*, Vol. 6 No. 1 pp 113-124, March 2005.
- [12] P. B. Tzvi, A. A. Goldenberg, J. W. Zu, "Design, Simulations and Optimization of a Tracked Mobile Robot Manipulator with Hybrid Locomotion and Manipulation Capabilities" *Proceedings. of IEEE International Conference on Robotics and automation*, pp 2307-2312. 2008
- [13] X. Wu, P. Lou, D. Tang, J. Yu, "An Intelligent-Optimal Predictive Controller for Path Tracking of Vision-based Automated Guided Vehicle" *Proceedings. of IEEE International Conference on Information and Automation*, pp 844-849, 2008.
- [14] C. Knospe, "PID Control" *IEEE Control Systems Magazine*, February 2006, pp. 30-31.
- [15] B.P. Nagaraj, R. Pandiyan, A. Ghoshal, "Kinematics of Pantograph Masts" *Mechanism and Machine Theory* Vol. 44 pg. no. 822-834, 2009.